Fast Strain Estimation and Frame Selection in Ultrasound Elastography using Machine Learning

Abdelrahman Zayed, *Student Member, IEEE* and Hassan Rivaz, *Senior Member*, *IEEE*

This supplementary material provides results that are complementary to those in the paper. We investigate the effect of changing the hyperparameter N, which refers to the number of principal components used, for both phantom and *in vivo* data. We also simulate the effect of changing the hyperparameter p, which refers to the number of RF lines used for extracting the sparse features. Depending on the rate of change of the displacement image in the horizontal direction, different values of p are needed.

Using the simulation data, we also show that our method works for different compression levels. In addition, we perform an experiment where we give out-of-plane RF frame pairs (i.e. poor) to the multi-layer perceptron classifier, to see whether it can correctly classify them as bad pairs.

Finally, we perform an experiment to show that it is acceptable to only compute the lateral displacement for p RF lines, followed by bi-linear interpolation, as compared to the more computationally expensive solution of calculating the displacement of all RF lines. We compare the axial strain produced by GLUE while providing it with an initial lateral displacement using both methods.

I. RESULTS

We used different number of principal components for both phantom and *in vivo* datasets to justify our choice of $N = 12$. Fig. 1, 2 and 3 show that $N = 6$ is a choice that works for all the datasets except the *in vivo* dataset after ablation. Therefore, we set $N = 12$ for our experiments. Fig. 4, 5 and 6 show that $p = 2$ is also a choice that works for all the datasets except the *in vivo* dataset after ablation. Therefore, we set $p = 5$ since it doesn't noticeably increase the computational complexity.

Tables I and II show a comparison between the signal to Noise Ratio (SNR) and Contrast to Noise Ratio (CNR) of both PCA-GLUE and GLUE for different levels of compression from 1% to 6%. In addition, we collected new data where the probe displacement is completely out-of-plane, trying to mimic an inexperienced user. We found that out of a total of 160 out-of-plane RF frame pairs, our classifier only chose 11 pairs as suitable for elastography, achieving an accuracy of 93.125%. This shows the ability of our classifier to distinguish the RF frames collected by an inexperienced user. Fig. 7 shows 3 of the 11 cases that were classified as suitable RF pairs. Although the compression was not in the axial direction, the displacement images are not completely out-of-plane.

We also compare our approach to the more computationally expensive method where the lateral displacement images given to GLUE are obtained by passing on all RF lines. Figs. 8, 9

TABLE I: The CNR values of the axial strain images for the simulation data at different compression levels.

Compression level	GLUE	PCA-GLUE
1%	**21.56**	19.74
3%	**21.59**	20.23
6%	**22.06**	19.58

TABLE II: The SNR values of the axial strain images for the simulation data at different compression levels.

Compression level	GLUE	PCA-GLUE
1%	22.58	**22.86**
3%	**25.47**	23.53
6%	**28.38**	27.98

and 10 show that the 2 methods yield the same results on both phantom and *in vivo* datasets.

(a) B-mode   (b) Strain using $N = 6$ (c) Strain using $N = 12$ (d) Strain using $N = 24$
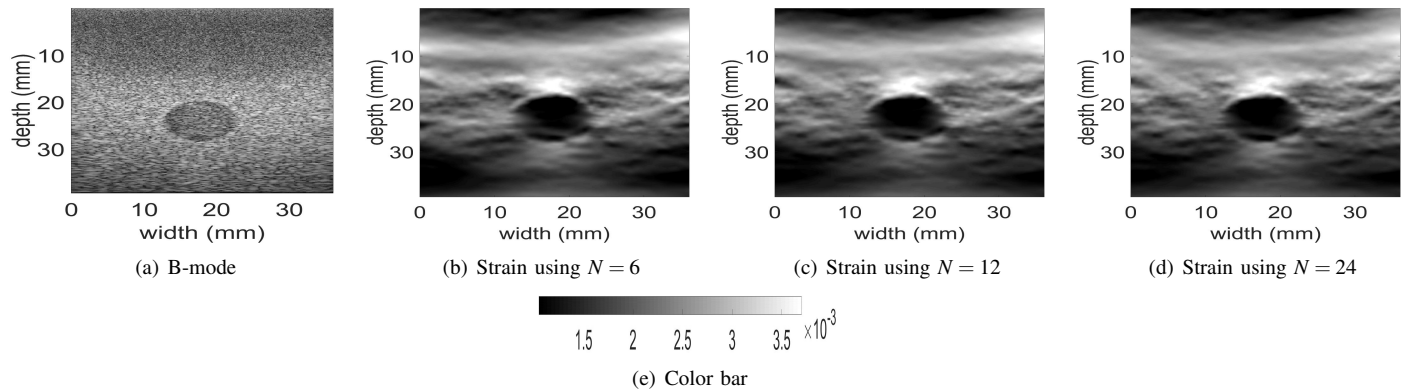
(e) Color bar

Fig. 1: The B-mode ultrasound and axial strain image using PCA-GLUE for the real phantom experiment as we increase the number of principal components N from 6 to 24. The color bar is for the strain images only.
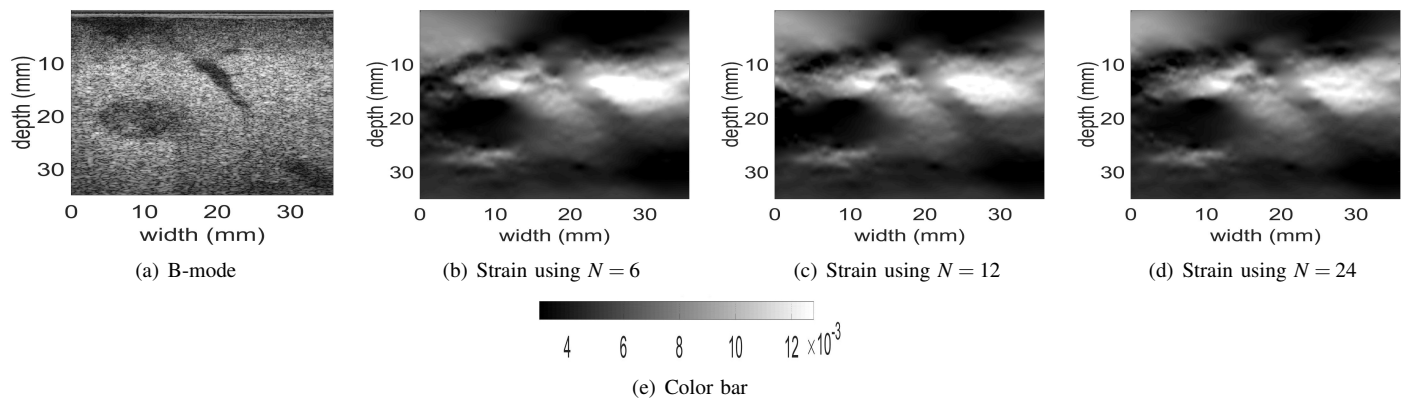

(a) B-mode   (b) Strain using $N = 6$ (c) Strain using $N = 12$ (d) Strain using $N = 24$

(e) Color bar

Fig. 2: The B-mode ultrasound and axial strain image using PCA-GLUE for the *in vivo* liver data before ablation as we increase the number of principal components N from 6 to 24. The color bar is for the strain images only.

(a) B-mode   (b) Strain using $N = 6$ (c) Strain using $N = 12$ (d) Strain using $N = 24$
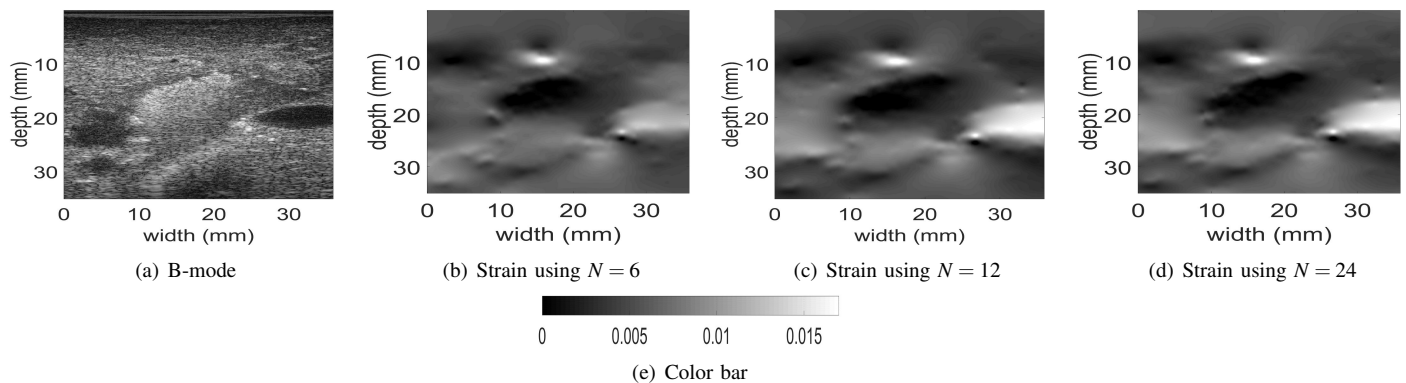
(e) Color bar

Fig. 3: The B-mode ultrasound and axial strain image using PCA-GLUE for *in vivo* liver data after ablation as we increase the number of principal components N from 6 to 24. The color bar is for the strain images only.

(a) B-mode   (b) Strain using $p = 2$ (c) Strain using $p = 5$ (d) Strain using $p = 10$
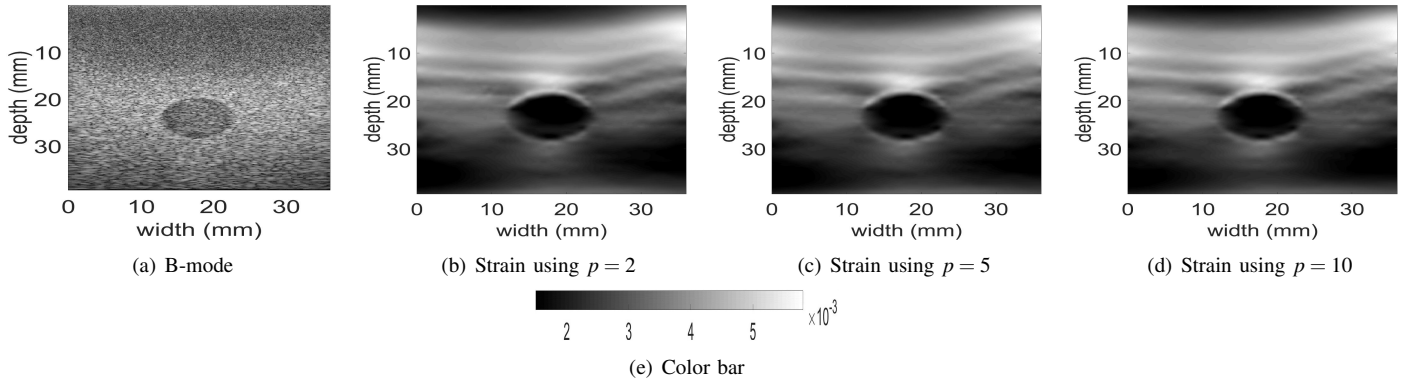
(e) Color bar

Fig. 4: The B-mode ultrasound and axial strain image using PCA-GLUE for the real phantom experiment as we increase the number of RF lines p from 2 to 10. The color bar is for the strain images only.

(a) B-mode   (b) Strain using $p = 2$ (c) Strain using $p = 5$ (d) Strain using $p = 10$
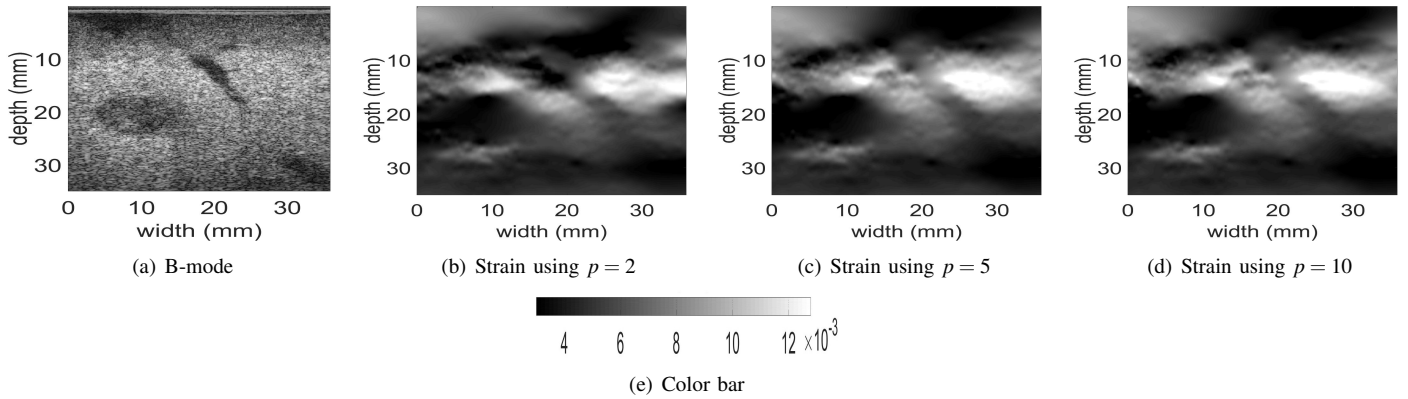
(e) Color bar

Fig. 5: The B-mode ultrasound and axial strain image using PCA-GLUE for the *in vivo* liver data before ablation as we increase the number of RF lines p from 2 to 10. The color bar is for the strain images only.

(a) B-mode   (b) Strain using $p = 2$ (c) Strain using $p = 5$ (d) Strain using $p = 10$
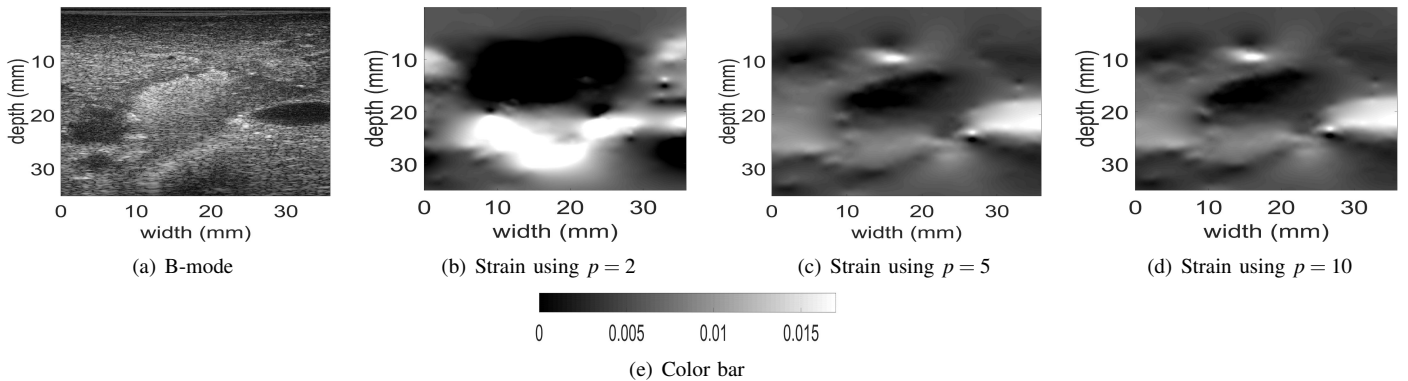
(e) Color bar

Fig. 6: The B-mode ultrasound and axial strain image using PCA-GLUE for *in vivo* liver data after ablation as we increase the number of RF lines p from 2 to 10. The color bar is for the strain images only.
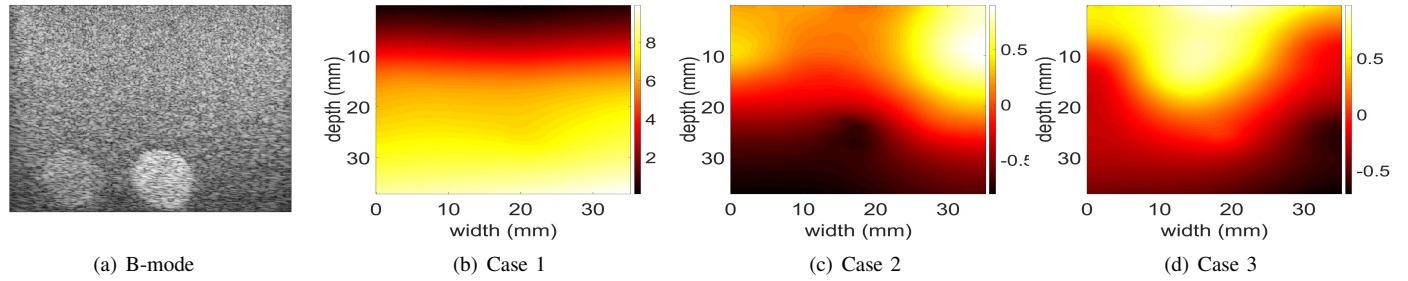
(a) B-mode   (b) Case 1   (c) Case 2   (d) Case 3

Fig. 7: Some of the displacement images incorrectly classified as suitable for elastography.

(a) B-mode   (b) Strain using method 1   (c) Strain using method 2
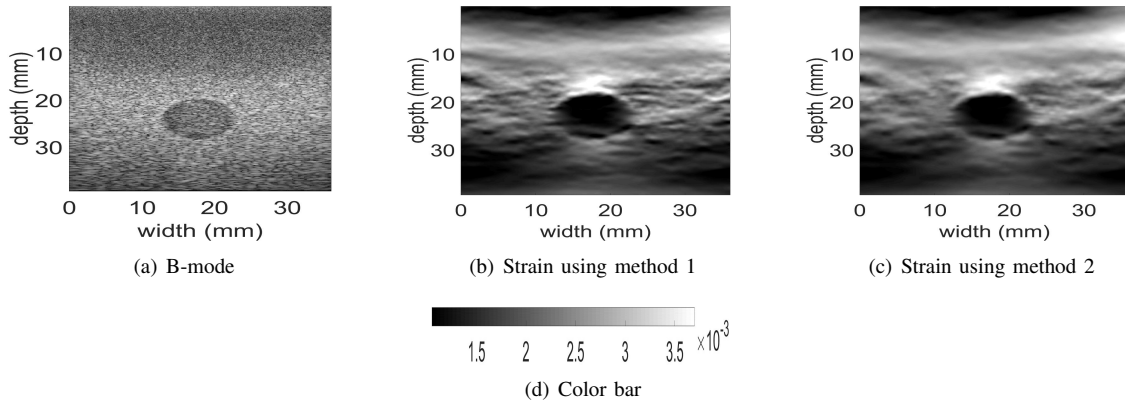
(d) Color bar

Fig. 8: A comparison between the axial strain estimated using 2 methods for the phantom experiment. In method 1, the lateral displacement given to GLUE is obtained by passing on all RF lines. In the method 2, the lateral displacement given to GLUE is obtained by passing only on 5 RF lines, followed by bi-linear interpolation. The color bar is for the strain images only.

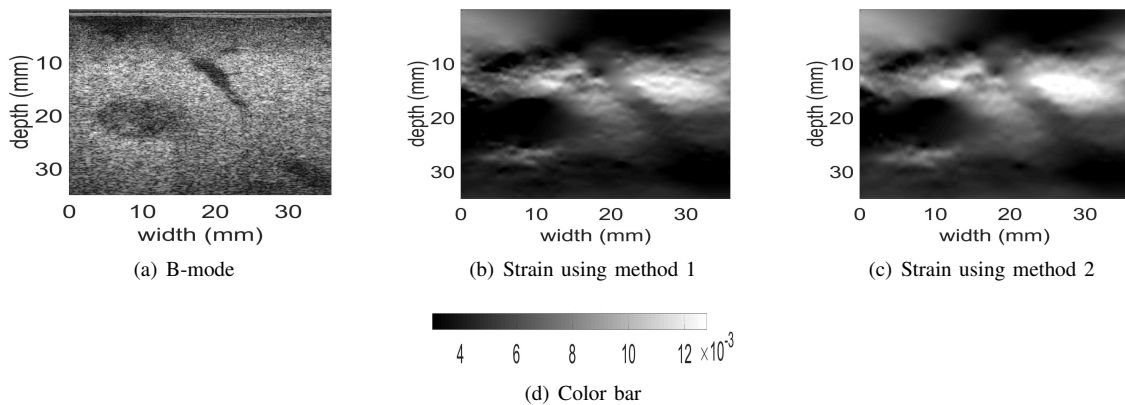(a) B-mode   (b) Strain using method 1   (c) Strain using method 2

(d) Color bar

Fig. 9: A comparison between the axial strain estimated using 2 methods for the *in vivo* liver data before ablation. In method 1, the lateral displacement given to GLUE is obtained by passing on all RF lines. In method 2, the lateral displacement given to GLUE is obtained by passing only on 5 RF lines, followed by bi-linear interpolation. The color bar is for the strain images only.

(a) B-mode

(b) Strain using method 1
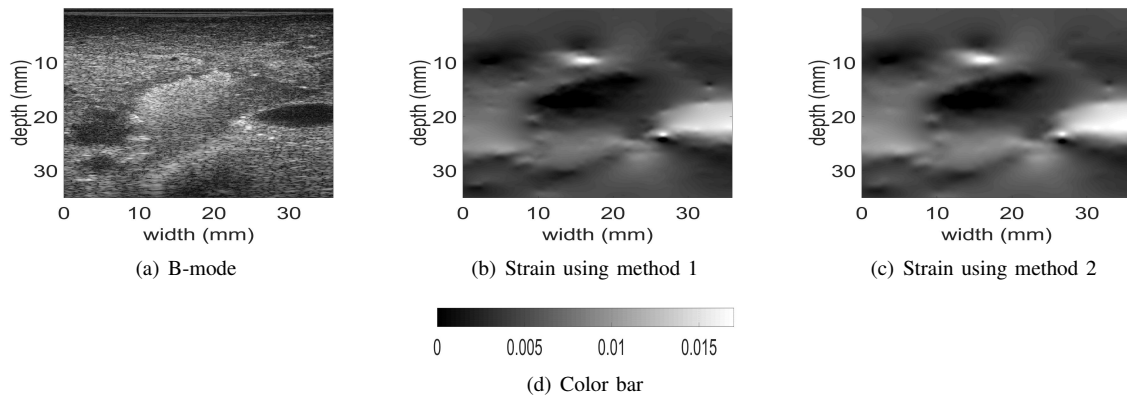
(c) Strain using method 2

(d) Color bar

Fig. 10: A comparison between the axial strain estimated using 2 methods for the *in vivo* liver data after ablation. In method 1, the lateral displacement given to GLUE is obtained by passing on all RF lines. In method 2, the lateral displacement given to GLUE is obtained by passing only on 5 RF lines, followed by bi-linear interpolation. The color bar is for the strain images only.